

# Development and validation of a non-linear $k$ - $\varepsilon$ model for flow over a full-scale building

N.G. Wright<sup>†</sup> and G.J. Easom<sup>‡</sup>

*School of Civil Engineering, The University of Nottingham, Nottingham NG7 2RD, U.K.*

R.J. Hoxey<sup>‡†</sup>

*Environment Group, Silsoe Research Institute, Wrest Park Silsoe Bedford MK45 4HS, U.K.*

**Abstract.** At present the most popular turbulence models used for engineering solutions to flow problems are the  $k$ - $\varepsilon$  and Reynolds stress models. The shortcoming of these models based on the isotropic eddy viscosity concept and Reynolds averaging in flow fields of the type found in the field of Wind Engineering are well documented. In view of these shortcomings this paper presents the implementation of a non-linear model and its evaluation for flow around a building. Tests were undertaken using the classical bluff body shape, a surface mounted cube, with orientations both normal and skewed at  $45^\circ$  to the incident wind. Full-scale investigations have been undertaken at the Silsoe Research Institute with a 6 m surface mounted cube and a fetch of roughness height equal to 0.01 m. All tests were originally undertaken for a number of turbulence models including the standard, RNG and MMK  $k$ - $\varepsilon$  models and the differential stress model. The sensitivity of the CFD results to a number of solver parameters was tested. The accuracy of the turbulence model used was deduced by comparison to the full-scale predicted roof and wake recirculation zone lengths. Mean values of the predicted pressure coefficients were used to further validate the turbulence models. Preliminary comparisons have also been made with available published experimental and large eddy simulation data. Initial investigations suggested that a suitable turbulence model should be able to model the anisotropy of turbulent flow such as the Reynolds stress model whilst maintaining the ease of use and computational stability of the two equations models. Therefore development work concentrated on non-linear quadratic and cubic expansions of the Boussinesq eddy viscosity assumption. Comparisons of these with models based on an isotropic assumption are presented along with comparisons with measured data.

**Key words:** turbulence model; wind engineering; anisotropy; full-scale; bluff body; computational fluid dynamics; buildings;  $k$ - $\varepsilon$ .

---

## 1. Introduction

Advances in computational techniques and technology have enabled the use of Computational Fluid Dynamics (CFD) in solving fluid flow problems in the field of wind engineering. Nevertheless the direct numerical simulation of practical turbulent fluid flows using the time dependent Navier

---

<sup>†</sup> Lecturer

<sup>‡</sup> Ph. D. Student

<sup>‡†</sup> Group Leader

Stokes equations in their simplest form is well beyond the capabilities of present day computing power. Consequently a number of turbulence models that attempt to model the effects of Reynolds stresses on the mean flow have been developed. Many of these turbulence models are commercially available and have been used successfully in aeronautical and mechanical engineering applications. The same is not true of wind engineering applications in which flow fields are highly complex and are characterised by the presence of multiple recirculation zones embedded within a uni-directional flow. The addition of streamline curvature and favourable and adverse pressure gradients leads to flow fields possessing very different turbulence scales and structures. The popular models employ representations of a length and velocity scale and are based on Reynolds averaging and the concept of an isotropic eddy viscosity. Consequently such models have great difficulty in simulating what are essentially transient and highly anisotropic flow fields. It is therefore apparent that one of the main obstacles to the use of CFD in wind engineering is that of turbulence modelling.

In view of these shortcomings the aim of the work presented here is to conduct research into the various methods available with a view to developing improved computational models for wind engineering. Earlier work (Wright and Easom 1999) concentrated on analysing the effects of the commonly available turbulence models, grid resolution, differencing schemes and boundary conditions on the accuracy of the results obtained from computational fluid dynamics simulations. Results obtained from these investigations have clearly shown the essential requirements for turbulence models to adequately predict bluff body flow fields. The findings will be discussed in detail later in this paper but mainly relate to the ability of the revised models to provide an adequate representation of turbulence anisotropy.

## 2. Theoretical aspects of CFD

In this work a finite volume technique is used to solve the Reynolds-averaged Navier-Stokes equations. The computational domain is divided into blocks, each with its own boundary fitted, structured grid. The blocks are connected at the interfaces between them and the solution technique iterates over each block until a converged solution is obtained.

For each block the velocity components are calculated sequentially and a derived pressure equation is solved according to the SIMPLE algorithm (Patankar and Spalding 1972). The solution of the system of linear algebraic equations can be carried out with several methods. Stones' Strongly Implicit method (Stone 1968) and an algebraic multigrid method (Webster 1998) have been used here. A higher order discretisation is used based on experience from earlier tests (Wright and Easom 1999).

A commercially available code - CFX (CFX International 1997) - is used and where necessary use is made of the ability to add user-defined FORTRAN subroutines to accomplish specific tasks. The implementation of the non-linear  $k$ - $\epsilon$  model is done through access to the source code. This route was taken, as opposed to the development of a bespoke code, to allow use of the existing tools for pre- and post-processing and to enable faster development of the new model.

Several turbulence models are implemented in CFX. Wright and Easom (1999) have previously evaluated the RNG and standard  $k$ - $\epsilon$  models and a modified  $k$ - $\epsilon$  model (Tsuchiya 1996). The differential stress model (DSM) was also tested to assess the accuracy of a fully anisotropic turbulence model. The results of this work showed very clearly the need for improved turbulence modelling in computational wind engineering. It was clear that the ability to model the anisotropy of turbulence was very important but perhaps equally important was the ability to apply a turbulence

model successfully to a wide range of complex flows. It was also apparent that the method of making ad-hoc modifications to the turbulence models was not satisfactory as general improvements in the flow field were not consistent at all points in the flow or for cases beyond the one initially used for validation. The more universal models such as the DSM appeared to suffer from severe numerical instability particularly when used in conjunction with higher order convection differencing schemes. Therefore an improved model should be able to model anisotropic turbulence, have universal applicability and have good numerical stability, i.e., incorporate the best features of both the DSM and the standard  $k-\varepsilon$  model. Following an extensive literature search the non-linear expansions of the Boussinesq hypothesis appeared to offer the best solution to the problem. Large eddy simulation techniques also appear promising, but impose severe computational requirements. Below the details of the non-linear approach are given. For more detail on the  $k-\varepsilon$ , RNG and DSM reference is made to earlier work (Wright and Easom 1999).

### 2.1. Revisions to the Boussinesq hypothesis - The non-linear $k-\varepsilon$ model

The effective viscosity hypothesis relates the Reynolds stresses solely to the rates of strain of the fluid and to scalar quantities. Boussinesq proposed the first effective viscosity hypothesis as early as 1877 (Boussinesq 1877). This formula, which simply represents the action of the  $u'w'$  shear stress, has been used with considerable success by, among others Ng (1971) and Rodi (1972) for free shear flows in turbulence models such as the standard  $k-\varepsilon$  model. Nonetheless, it has been observed that the Boussinesq hypothesis fails in a number of applications including boundary layers over curved surfaces. Bradshaw (1973, 1992) has stated that this failure is due to the form of the stress strain relation rather than the inapplicability of the eddy viscosity approach.

In order to account for flows in which more than one Reynolds stress is required to fully describe a given flow field the Boussinesq hypothesis is generalised to give the isotropic eddy viscosity assumption used in the majority of turbulence models. The standard and revised Boussinesq hypothesis, used in the standard  $k-\varepsilon$  model are detailed in Eqs. (1) and (2).

$$\tau_{ij} = -\rho \overline{u'_i u'_j} = \mu_t \left( \frac{\partial u_i}{\partial x_j} + \frac{\partial u_j}{\partial x_i} \right) \quad (1)$$

$$-\rho \overline{u'_i u'_j} = \mu_t \left( \frac{\partial u_i}{\partial x_j} + \frac{\partial u_j}{\partial x_i} \right) - \frac{2}{3} \rho k \delta_{ij} \quad (2)$$

This theory is invalid for flows in which  $u'u' \neq v'v' \neq w'w'$ . The first attempts to remove this deficiency in the eddy viscosity assumption were undertaken by Lumley (1970). Pope (1975) adopted a similar approach to Lumley in formulating a constitutive relation for the Reynolds stresses resulting in a finite tensor polynomial to form a revised general effective viscosity hypothesis. Pope proposed a new model of eddy viscosity that could capture normal stress anisotropy and overcome the limitations of the standard formulation.

Others authors (Speziale 1987, Suga 1996, Craft *et al.* 1996) have made revisions to the anisotropic eddy viscosity relationship to allow its use in computational models applied to a wide range of three dimensional turbulent flows. Craft *et al.* have proposed both quadratic and cubic expansions of the Boussinesq hypothesis as follows :

Quadratic :

$$\begin{aligned}
 u_i u_j = & -\mu_t S_{ij} + \frac{2}{3} \delta_{ij} k \\
 & + C_1 \mu_t \frac{k}{\varepsilon} \left( S_{ik} S_{kj} - \frac{1}{3} S_{ik} S_{kl} \delta_{ij} \right) \\
 & + C_2 \mu_t \frac{k}{\varepsilon} (\Omega_{ik} S_{kj} + \Omega_{ik} S_{ki}) \\
 & + C_3 \mu_t \frac{k}{\varepsilon} \left( \Omega_{ik} \Omega_{jk} - \frac{1}{3} \Omega_{lk} \Omega_{lk} \delta_{ij} \right)
 \end{aligned} \tag{4}$$

where :

$$S_{ij} = \left( \frac{\partial u_i}{\partial x_j} + \frac{\partial u_j}{\partial x_i} \right) \quad \text{and} \quad \Omega_{ij} = \left( \frac{\partial u_i}{\partial x_j} - \frac{\partial u_j}{\partial x_i} \right)$$

Cubic :

$$\begin{aligned}
 u_i u_j = & -\mu_t S_{ij} + \frac{2}{3} \delta_{ij} k \\
 & + C_1 \mu_t \frac{k}{\varepsilon} \left( S_{ik} S_{kj} - \frac{1}{3} S_{ik} S_{kl} \delta_{ij} \right) \\
 & + C_2 \mu_t \frac{k}{\varepsilon} (\Omega_{ik} S_{kj} + \Omega_{ik} S_{ki}) \\
 & + C_3 \mu_t \frac{k}{\varepsilon} \left( \Omega_{ik} \Omega_{jk} - \frac{1}{3} \Omega_{lk} \Omega_{lk} \delta_{ij} \right) \\
 & + C_4 \mu_t \frac{k^2}{\varepsilon^2} (S_{ki} \Omega_{lj} + S_{kj} \Omega_{li}) S_{kl} \\
 & + C_5 \mu_t \frac{k^2}{\varepsilon^2} \left( \Omega_{il} \Omega_{lm} + S_{il} \Omega_{lm} \Omega_{mj} - \frac{2}{3} S_{lm} \Omega_{mn} \Omega_{nl} \delta_{ij} \right) \\
 & + C_6 \mu_t \frac{k^2}{\varepsilon^2} S_{ij} S_{kl} S_{kl} \\
 & + C_7 \mu_t \frac{k^2}{\varepsilon^2} S_{ij} \Omega_{kl} \Omega_{kl}
 \end{aligned} \tag{5}$$

The coefficients  $C_1$  to  $C_7$  have been derived from considering the prediction of the stresses from a wide range of turbulent flows. The first term on the right in Eq. (5) is the standard approximation. It can be seen that the addition of up to a further seven terms makes the relationship a great deal more mathematically complex. These additional terms which are quadratic and cubic in the mean velocity gradients (Wilcox 1994). Detailed tests by Speziale (1988) have shown that the quadratic model gives significantly improved predictions for the reattachment length of the separated region behind the backward facing step, with results similar in accuracy to that obtained using a Reynolds stress model. Furthermore, the non-linear quadratic model successfully predicted an eight vortex secondary flow in the non circular duct, an occurrence usually only predicted by second order closure models which are able to predict the individual Reynolds stresses. The quadratic models are designed for problems in which flow anisotropies are the distinguishing feature. The cubic model includes extra terms in the constitutive relation between Reynolds stresses and strain rates so it is reported to give better predictions in curved flows, for example, over curved surfaces including hills. Therefore it

could be argued that the quadratic model should be sufficient to describe the flow in a majority of wind engineering bluff body simulations.

Due to the nature of the non-linear model, comparisons have been made with the second order closure, algebraic stress model. There is a similarity in both models in that the stresses are linked non-linearly to all strain components, but beyond this the two models are very different as the algebraic stress model is based on simplified transport terms for the full Reynolds stress equations.

In a similar manner to the  $k$  and  $\varepsilon$  equations and the Reynolds stress transport equations detailed earlier, the non-linear models are rigorously derived from either the Navier-Stokes equations or the eddy viscosity Boussinesq hypothesis. The authors are of the opinion that turbulence models of this kind, rather than turbulence models modified in an ad-hoc manner, are the most sensible way to improve the current modelling technology.

Reported deficiencies and errors with these models are particularly scarce due to the small amount of testing undertaken in this field. Nevertheless it has been reported that the cubic non-linear model is the preferred expansion due to the fact that it can be applied to a greater range of flow fields, including curved surfaces (Craft *et al.* 1996). As such the model constants used to close the equations can be calibrated from a much wider range of flows thus making the model more universally applicable than the quadratic model. In addition, it should be noted that the algebraic expressions for the Reynolds stresses are unable to model fluid transport effects as can the differential stress model.

## 2.2. Turbulence model validation

Since the 1980 AFOSRenHTTM Stanford conference on complex turbulent flows the two-dimensional backward facing step has been established as a standard method of validating turbulence model performance and accuracy. Therefore this provided the ideal test case for the new turbulence models.

Basora and Younis (1992) have previously compared standard  $k-\varepsilon$  model results with wind tunnel based 2D back-step tests undertaken by Kim *et al.* (1980). The standard  $k-\varepsilon$  model results produced by CFX4 were found to be the same as those found by Basora. The revised turbulence models were then compared with the experimental data. Table 1 shows the results. The Speziale (1987) quadratic non-linear turbulence model was tested for this case but could not provide converged solutions. It is reported that there are general convergence problems due to high gradients returned by the second derivatives of velocity brought about by the use of the Oldroyd derivative term, see Eq. (8) (Speziale and Ngo 1988). As such this model was not tested further.

Preliminary testing of the DSM with the Gibson and Launder (1978) wall reflection terms for the

Table 1 Reattachment lengths for backward facing step ( $h =$  step height)

Turbulence model	Reattachment. length
Std $k-\varepsilon$	$5.4h$
Non-linear quadratic (Speziale)	-----
Non-linear quadratic (UMIST)	$6.5h$
Non-linear cubic (UMIST)	$7.15h$
DSM (no wall reflection)	$6.5h$
DSM (wall reflection terms)	-----
Experimental (Kim <i>et al.</i> 1980)	$7.0h$

2D back-step test case was unsuccessful. The addition of these terms as sources to the Reynolds stress transport equation resulted in extremely poor numerical stability and a resulting lack of convergence.

Comparisons between the standard  $k-\varepsilon$  and Craft *et al.* quadratic non-linear  $k-\varepsilon$  models show no measurable difference in solution times. The extra time required per iteration of the non-linear model was offset by an increase in the speed of convergence, as this model avoids the unrealisable values returned by the production of the turbulent kinetic energy term in the standard  $k-\varepsilon$  model. In terms of the accuracy of the models tested it can be seen that the standard  $k-\varepsilon$  model predicts the worst results with an error of approximately 23 percent. This was followed by the DSM and then the quadratic and cubic non-linear  $k-\varepsilon$  models with errors of 7 and 2 percent respectively. These initial results combined with extensive checking of the code alterations effectively validated the revised models and give an early indication of possible improvements in the predicted flow fields.

### 3. Test case

#### 3.1. Details of the tests

The CFD testing for this project used the well documented case of flow around a three dimensional surface mounted cube in an atmospheric boundary layer, with comparisons carried out at full-scale rather than the usual wind tunnel scale. Cube orientations normal and skewed at  $45^\circ$  to the incident wind have been analysed. Subsequently full comparisons of experimental and computationally derived results have been undertaken with the results obtained from testing of a 6 m cube located at the Silsoe Research Institute (see Hoxey *et al.* 1999 for full details).

The computational domain was designed so as to reduce to a minimum the interference with the flow field around the cube. Fig. 1 shows the domain size and boundary conditions. Baetke *et al.* (1990) states that the blockage ratio, defined as the ratio of the frontal area of the cube to the

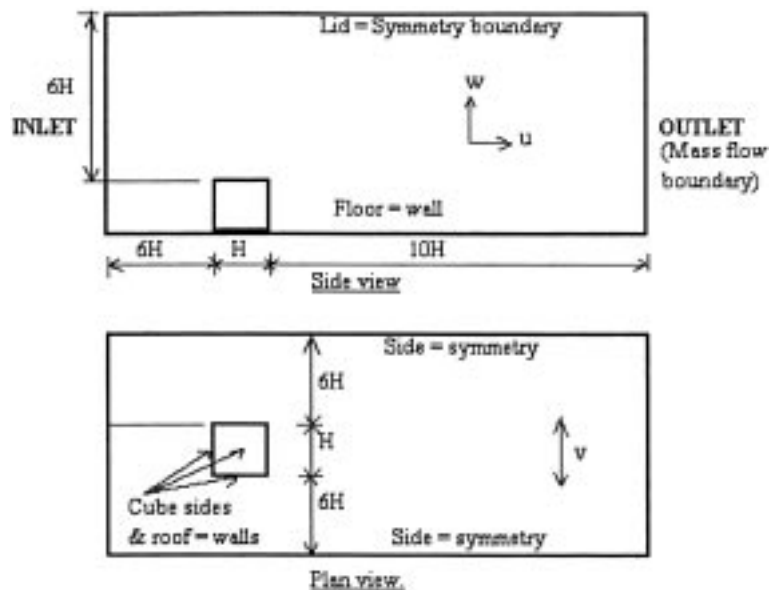


Fig. 1 Geometry and boundary conditions

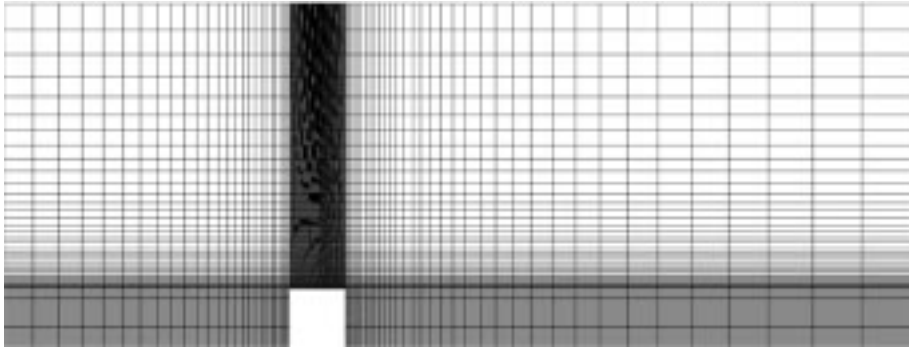


Fig. 2 Example grid to show refinement in vicinity of building

vertical cross sectional area of the computational domain should be no greater than 3 percent. The blockage ratio for these tests was less than half this value. Furthermore flow gradients at the outlet were investigated to determine a suitable length of the computational domain for the wake region so as not to compromise the interior solution accuracy of the simulation. Approximately 120,000 cells were used in meshing the domain with particular attention paid to areas of high flow gradients at the areas of flow impingement and separation. Fig. 2 shows the grid and demonstrates the refinement in the vicinity of the buildings. Grid independence tests were completed utilising finite volume meshes with up to 1.25 million cells and between 20 and 90 cells along the building side. With regards to the normal cube, grid refinements improved the accuracy of the roof flow field by approximately 10 percent although no difference was found for the remaining faces of the cube. Noteworthy results were found for the cube skewed at  $45^\circ$  to the incident wind. Although no changes in the results were apparent for the windward and leeward faces of the cube the roof windward edge peak negative pressures were found to increase markedly with refinements of the grid. Discussions with Hoxey (1999) suggest that in this region the delta wing vortices are approximately 400 mm in diameter and have a very high angular velocity. Adequate numerical resolution of this region with the 6 m cube model in the CFD simulation was consequently particularly difficult to obtain. The finest possible grid was used for these simulations utilising approximately 1 million nodes. An example of the effect of grid refinement can be seen in Fig. 3 where the strength of the delta wing vortices increased upon successive grid refinements.

In order to match the computational and experimental boundary layers the floor roughness length was set equal to 0.01 m to represent the fetch at the SRI and the cube walls were given a roughness length equal to 0.005 m. This was done through an amendment to the logarithmic law of the wall. The inlet conditions were generated by running the CFD simulations for flow over rough ground with no building present and periodic streamwise boundary conditions to give a velocity of 10 m/s at the building height. This gave fully developed equilibrium flow profiles including variables such as streamwise velocity and turbulent kinetic energy that were consistent with the floor roughness. These were used as inlet conditions for simulations with a building in the flow. The results returned by the numerical boundary layer simulations were in excellent agreement with Richards and Hoxey (1993) which details equations that specify the velocity profile and a maximum value of turbulent kinetic energy production at ground level.

Initially four turbulence models including the MMK (Tsuchiya *et al.* 1996), RNG (Yakhot *et al.* 1992) and standard  $k-\varepsilon$  (Lauder *et al.* 1974) model and the differential stress model (Lauder *et al.*

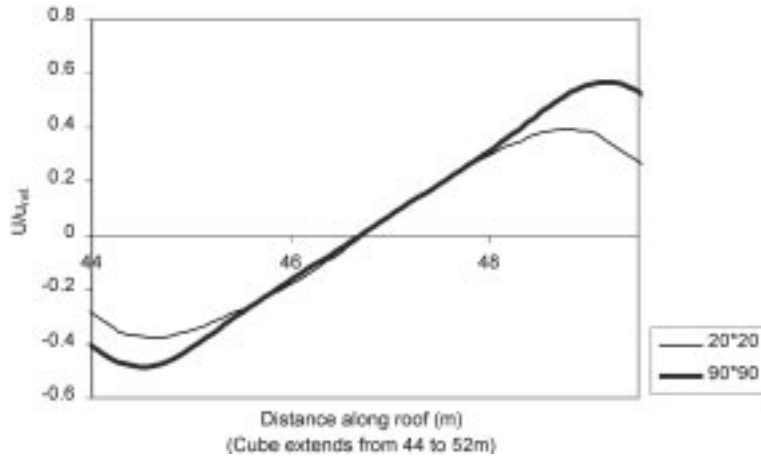


Fig. 3 Skewed cube, lateral velocity component over the roof with grid refinement

1975) were tested for both the cube normal and skewed at  $45^\circ$  to the incident wind. All the tests were repeated for both hybrid (Spalding 1972) and CCCT (Gaskell *et al.* 1988) convective differencing. The minimum residual reduction factors (the ratio of the first to last residual error values) achieved were  $10^5$  with a small number of tests achieving reduction factors of  $10^7$ . This paper highlights the results from pressure coefficients from the standard RNG and non-linear  $k-\epsilon$  models with additional flow field details supplied from the differential stress and MMK  $k-\epsilon$  models.

All flow calculations utilised the CFD package CFX. In this the Navier-Stokes equations are discretised using the finite volume method. Various methods are available in CFX to solve the system of linear algebraic equations. This work used Stones strongly implicit method and an algebraic multigrid method. The diffusion terms are discretised using central differencing and alternative discretisation schemes for the convection terms were tested as detailed earlier

## 4. Results

### 4.1. Roof and wake flow fields

Table 2 shows that the standard  $k-\epsilon$  model poorly simulates the mean flow field for the cube normal to the incident wind with no roof re-circulation predicted and an over prediction of the wake reattachment point. The MMK  $k-\epsilon$  model and the DSM also poorly predict the roof flow field

Table 2 Cube normal to incident wind ( $H$  = cube dimension)

Turbulence model	Roof reat.	Wake reat.
Standard $k-\epsilon$	none	2.2H
MMK. $k-\epsilon$	No reattach.	3.12H
RNG $k-\epsilon$	0.84H	2.5H
Non-lin. Quad., $k-\epsilon$	0.75H	2.15H
Differential stress.	No reattach.	2.0H
<b>Exp.</b> (S.R.I. 1999)	0.7H	1.2-1.4h

producing a roof re-circulation bubble that extended over the entire cube roof with no reattachment. Furthermore the MMK model seriously over predicts the size of the wake recirculation. The RNG  $k-\epsilon$  model appears to produce good results with the prediction of a roof re-circulation zone with reattachment and a shorter wake re-circulation zone. Overall the most accurate prediction was produced by the non-linear quadratic  $k-\epsilon$  model. It was not possible to obtain fully converged results with the cubic non-linear model when using this geometry.

The  $k-\epsilon$  model over predicts the turbulent kinetic energy at the windward face which excessively mixes the flow and arrests the vertical velocity component. This results in the flow remaining attached to the roof and a poor flow field prediction. A similar result was found for the skewed cube case.

The MMK  $k-\epsilon$  model shows a very different picture indeed with flow re-circulation occurring over the entire length of the roof with no flow reattachment. Fig. 9 shows the very small levels of turbulent kinetic energy produced by this model, which are a good deal smaller than all the other models tested. A beneficial consequence of this is the prediction of relatively strong delta wing vortices for the skewed cube orientation.

The RNG  $k-\epsilon$  model produces good results with a relatively accurate prediction of the roof and wake vortices. The turbulent kinetic energy production at the front face of the cube appears to be approximately half way between the DSM and the standard  $k-\epsilon$  model.

The DSM which is the most complex of all the models tested and is a fully anisotropic turbulence model produces surprisingly poor results for the roof flow field with no flow reattachment whatsoever.

#### 4.2. Pressure coefficient distribution: cube normal to the incident wind

The line positions shown in Figs. 4 and 5 indicate the locations used when recording data with CFX-Visualise linegraph and the general locations of the pressure taps for the full-scale experiments.

Fig. 6 shows the centreline windward face mean pressure coefficient distributions. It can be clearly seen that the standard  $k-\epsilon$  model over predicts the pressure distribution by approximately 25 to 30 percent at the flow stagnation point. The remaining four models all predict relatively similar results within approximately 10 percent of the experimentally obtained values. It is also apparent from the results that the CFD predicted stagnation point is approximately 0.5 m higher than that

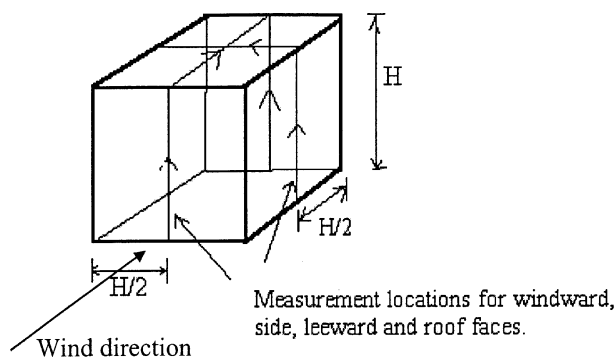


Fig. 4 Normal cube measurement locations

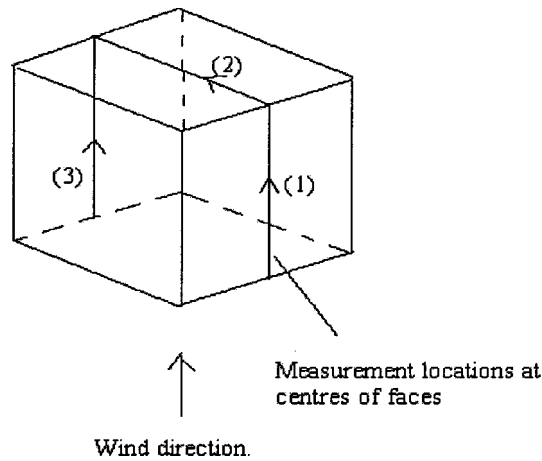


Fig. 5 Skewed cube measurement locations

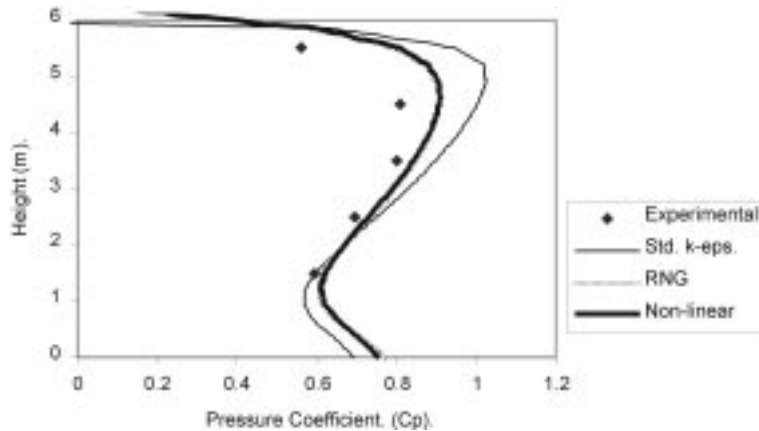


Fig. 6 Mean pressure coefficients for the windward face of the normal cube

obtained by experiment.

Fig. 7 shows the centreline pressure coefficient distributions for the roof of the cube. The non-linear quadratic model and the RNG model predict the most accurate peak pressures within 5 percent of the peak mean experimental values. The standard  $k-\epsilon$  model over predicts the peak pressure by approximately 50 percent. It is apparent that none of the models tested could accurately predict the pressure distribution over the remainder of the roof with even the best CFD results calculating errors of 20 to 30 percent. Grid refinement tests for the RNG and non-linear  $k-\epsilon$  models resulted in an overall improvement of 10 percent for the roof pressure predictions.

It should be noted that there is some question over the accuracy of the middle two experimental points :

‘The experimental results show there are a few inconsistent points for the pressure coefficient on the side wall, however for the roof there are patterns which cannot be fully explained and may be associated with the approach flow turbulence intensity variations. This is to be the subject of further

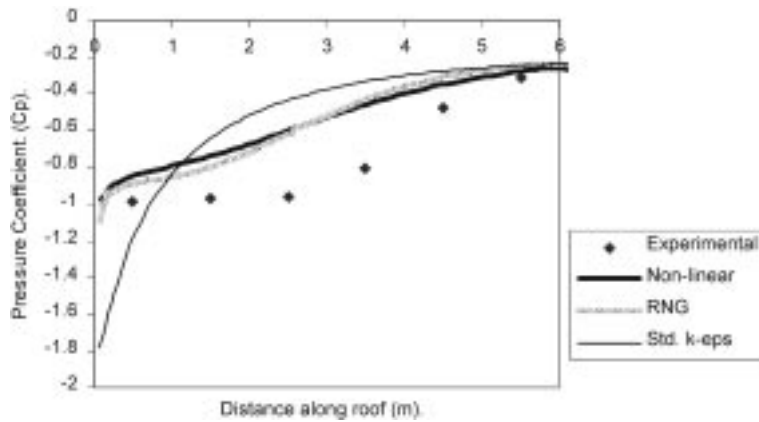


Fig. 7 Mean pressure coefficients for the roof of the normal cube

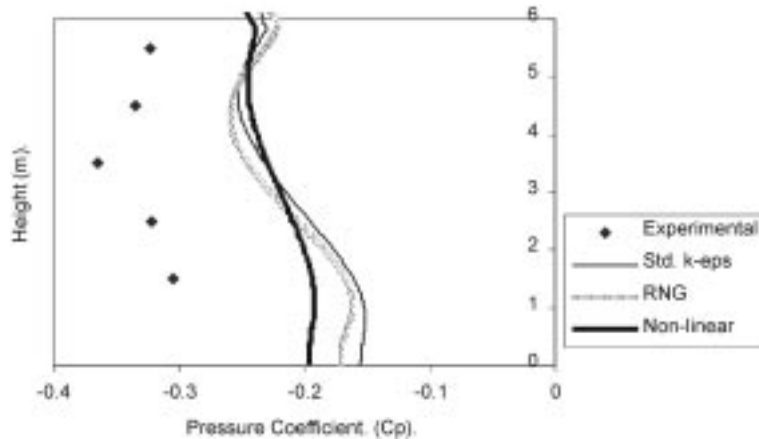


Fig. 8 Mean pressure coefficients for the leeward face of the normal cube

investigations.' (Hoxey *et al.* 1999).

Nonetheless the results here are not as good as might be hoped, although they do display the correct magnitude and trends.

The leeward pressure distributions can be seen on Fig. 8. With errors of approximately 30 to 35 percent it is again apparent that none of the models tested could accurately predict the experimentally obtained distribution. No improvement was found with grid refinement. There is again some question over the middle experimental value obtained which appears to be out of sequence with the remaining values. It appears that the under predictions of negative pressure are a consequence of the over prediction of the wake recirculation and the corresponding lack of velocity deficit. These results confirm the need to accurately predict the flow field around the bluff body.

The side face and lateral roof pressure distribution can be seen on Figs. 9 and 10 respectively. The experimental results for the side face show a slow increase in negative pressure as the wind velocity increases with height. It can be seen that this trend is well reproduced by the RNG  $k-\epsilon$  model but

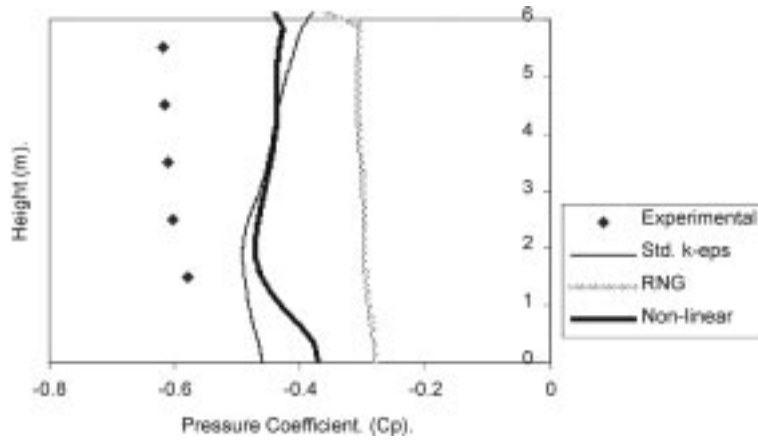


Fig. 9 Mean pressure coefficients for the side face of the normal cube

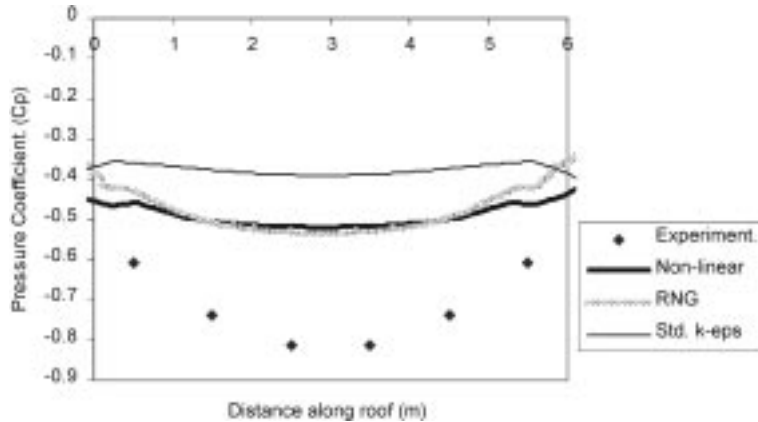


Fig. 10 Mean pressure coefficients for the roof of the normal cube, lateral measurement line

not so well by the remaining models. The standard  $k-\epsilon$  model predicts the highest negative pressures for the first 3 m height of the side face, possibly for the same reason that it fails to calculate flow recirculation over the roof of the cube, due to excessive prediction of turbulent kinetic energy as described below.

RNG predicts poorly for side wall and the standard  $k-\epsilon$  similarly for the roof. The non-linear model gives better results overall, but with errors in the side and roof pressure prediction ranging from 20 to 30 percent and 30 to 40 percent respectively. Fig. 10 further demonstrates the results shown by Fig. 7 highlighting the inability of the models tested to accurately calculate the pressure distribution over the roof of the cube. The trend shown by the experiment represents the reduction in size and strength of the roof recirculation zone as the sides of the cube are approached and the mass of air flowing over the roof is reduced. It is clear that the experimental results are affected to a much larger extent by this three dimensional phenomenon due to the significant difference between the centre and edge negative pressures. This perhaps suggests that the roof recirculation zone in the full scale experiments contains a much stronger vortex than that predicted by CFD. This would further explain the slow reduction in negative pressure as the roof is traversed as shown on Fig. 7.

#### 4.3 Pressure coefficient distribution: Cube skewed at $45^\circ$ to the incident wind

Fig. 11 shows the CFD and experimental pressure coefficient distribution for measurement location number 1. The standard  $k-\epsilon$  model again appears to over predict the mean pressure at the stagnation point, although with a lower error than for the normal cube due to the reduced flow impingement. The remaining models all calculated similar front face pressures with an error of approximately 25 percent. In addition, all the CFD models predict a flow stagnation point approximately 1.5 metres higher than that obtained from the full-scale experiment.

Fig. 12 shows the roof pressure distributions for measurement line 2. In this case the standard  $k-\epsilon$  model predicts the least negative pressures due to the prediction of very weak delta wing vortices. Successive refinements of the grid over the cube achieved a 15 percent increase in the peak pressure over the roof and improvements to the distribution of the pressures.

Referring to Fig. 13, which shows the predicted pressure distributions for measurement location number 3, it can be seen that the non-linear model calculates values marginally better than RNG with an error of approximately 40 percent. Furthermore this model calculated a relatively accurate

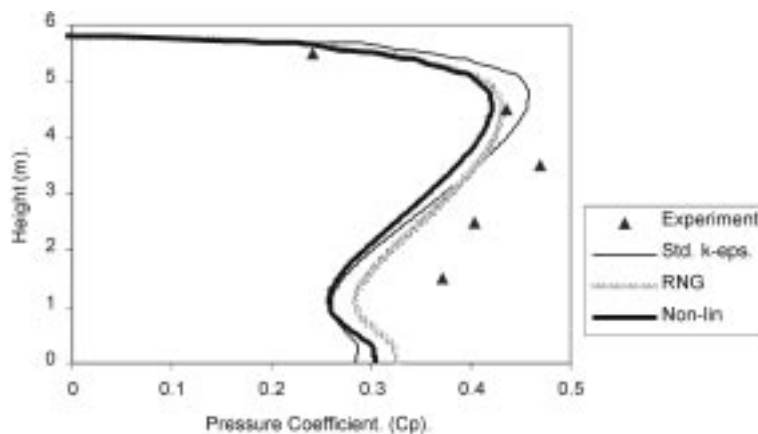


Fig. 11 Skewed cube windward face pressure distribution

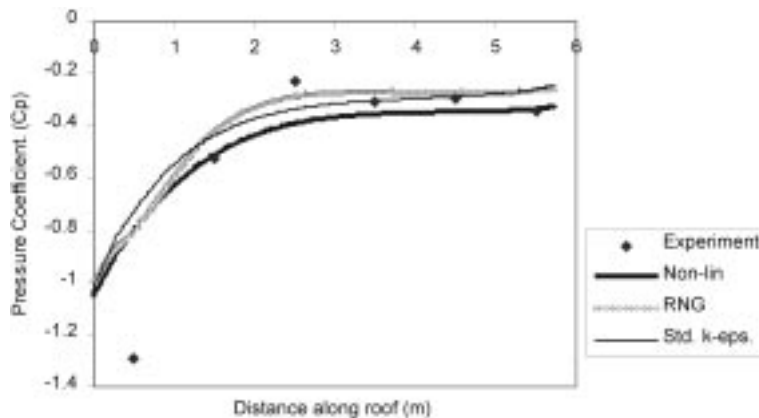


Fig. 12 Skewed cube roof pressure distribution

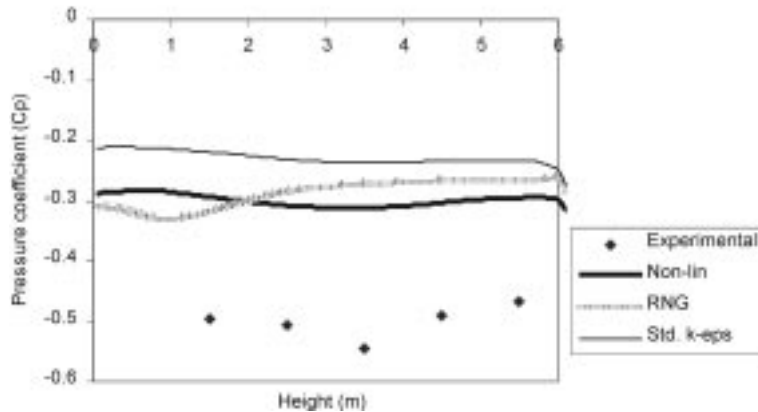


Fig. 13 Skewed cube leeward face pressure distribution

pressure distribution profile with a small increase at the centre of the cube. The standard  $k-\epsilon$  model again predicts the worst distribution with errors of up to 60 percent. None of the latter models correctly predicted the profile of mean pressure on the leeward face of the cube.

## 5. Discussion

From the results presented it is apparent that errors in the  $k-\epsilon$  model are due to the use of the isotropic eddy viscosity concept in a highly anisotropic flow field. The errors found with this model are mainly due to inaccurate prediction of turbulent kinetic energy levels. The excessive values of turbulent kinetic energy are caused by overestimation of the turbulence production term,  $P_k$ , which is a consequence of the eddy viscosity concept. The isotropic eddy viscosity formulation simply sums the turbulence production due to these terms. Hence eddy viscosity models which feature the turbulent energy transport equation tend to return excessive levels of energy and thus turbulent diffusion in the presence of strong compressive strain, as can be seen in Fig. 14. Referring to the wake region it is clear that the standard  $k-\epsilon$  model over predicts the size of the recirculation vortex. As this region exhibits strong turbulence anisotropy where the  $v'v'$  lateral Reynolds stress component dominates (Murakami 1993) it is immediately apparent that isotropic eddy viscosity models will not be able to adequately predict the recirculation vortex. This model underestimates the value of  $v'v'$  in the wake region and consequently underestimates the momentum diffusion in the lateral direction (Murakami 1993). The net result of this is that the kinetic energy, calculated as the sum of the Reynolds stress, is underestimated and thus the predicted value of eddy viscosity is too small. Insufficient mixing of the flow in the vortex results in an over prediction of the reattachment length and too large a velocity in the reverse flow. The skewed cube results for this model suffer in a similar manner.

Referring to the results obtained from the 6 m cube tests the RNG  $k-\epsilon$  model appears to produce good results particularly when compared to the performance of the standard  $k-\epsilon$  model. It is the only generally available turbulence model that is able to predict flow separation and reattachment on the roof of the cube which in turn produced an improved roof pressure distribution. Generally this model predicted relatively accurate pressure distributions for all sides of the normal and skewed cube.

Non-linear  $k-\epsilon$  models have been developed in an attempt to better incorporate the effects of

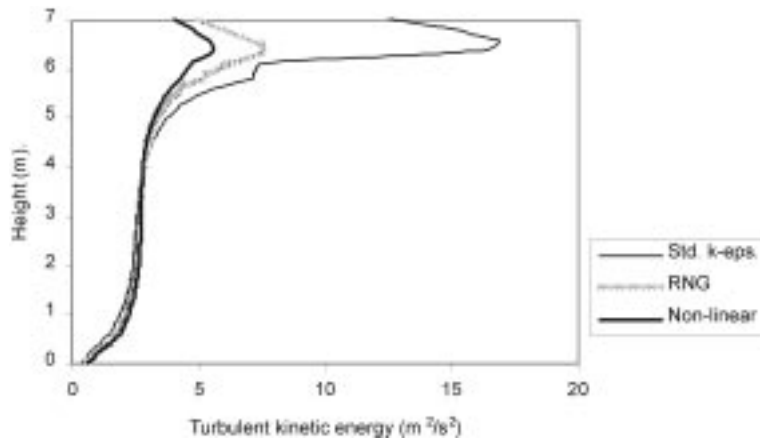


Fig. 14 Turbulent kinetic energy profile for the windward face

anisotropic turbulence and to try to obtain a width of applicability approaching that of second moment closure. The advantage of using non-linear expansions of the Boussinesq hypotheses to develop improved turbulence models is that it should produce universal improvements. This is in contrast to ad-hoc improvements, such as the MMK model that may improve predictions for a particular application of the model only. Furthermore non-linear models require much less computational effort, due to their improved stability characteristics. The overproduction of turbulent kinetic energy, as explained in the  $k-\varepsilon$  model results, is not an issue with this model, which uses the full kinetic energy production term.

The results highlighted show that for a number of cases the non-linear quadratic  $k-\varepsilon$  model appears to outperform the DSM both in terms of mean pressure distributions and predicted vortex dimensions. The fact that the more complex DSM does not necessarily perform any better than the simpler models is also stated by Menter and Grotjans (1999). It is also clear that improved predictions have been obtained with the non-linear model over the isotropic eddy viscosity models such as the RNG and standard  $k-\varepsilon$  models for all the majority of simulations undertaken in this study.

It has been reported by Murakami *et al.* (1996) that the DSM fails to predict reattachment of the roof vortex due to an underestimation of the  $u'w'$  shear stress at the front corner of the cube. Although absolute values are not available from the SRI experiments, Figs. 13 and 14 show that the non-linear model predicts markedly higher values of the shear stress at the front corner thus resulting in the more accurate vortex prediction. The reattachment of the roof vortex results in a marginally more accurate roof pressure distribution.

Figs. 15(a-c) demonstrate the abilities of the non-linear model to predict anisotropic stresses and correctly show the dominant stress over the roof to be the stream-wise Reynolds stress. Murakami states that the DSM accurately predicts the distribution and anisotropy of the Reynolds stresses over the roof of the cube and errors in both the eddy viscosity model and algebraic stress model are not reproduced. Figs. 16 and 17 show that there is a very similar distribution of stresses along the roof for both the DSM and non-linear models. Furthermore the non-linear model correctly predicts the lateral  $w'w'$  stress to be dominant in the wake region, see Fig. 18. This further validates the results from the non-linear model and highlights improved accuracy over the ASM and eddy viscosity models.

The prediction of the roof vortex size with the isotropic  $k-\varepsilon$  models is usually related to the levels

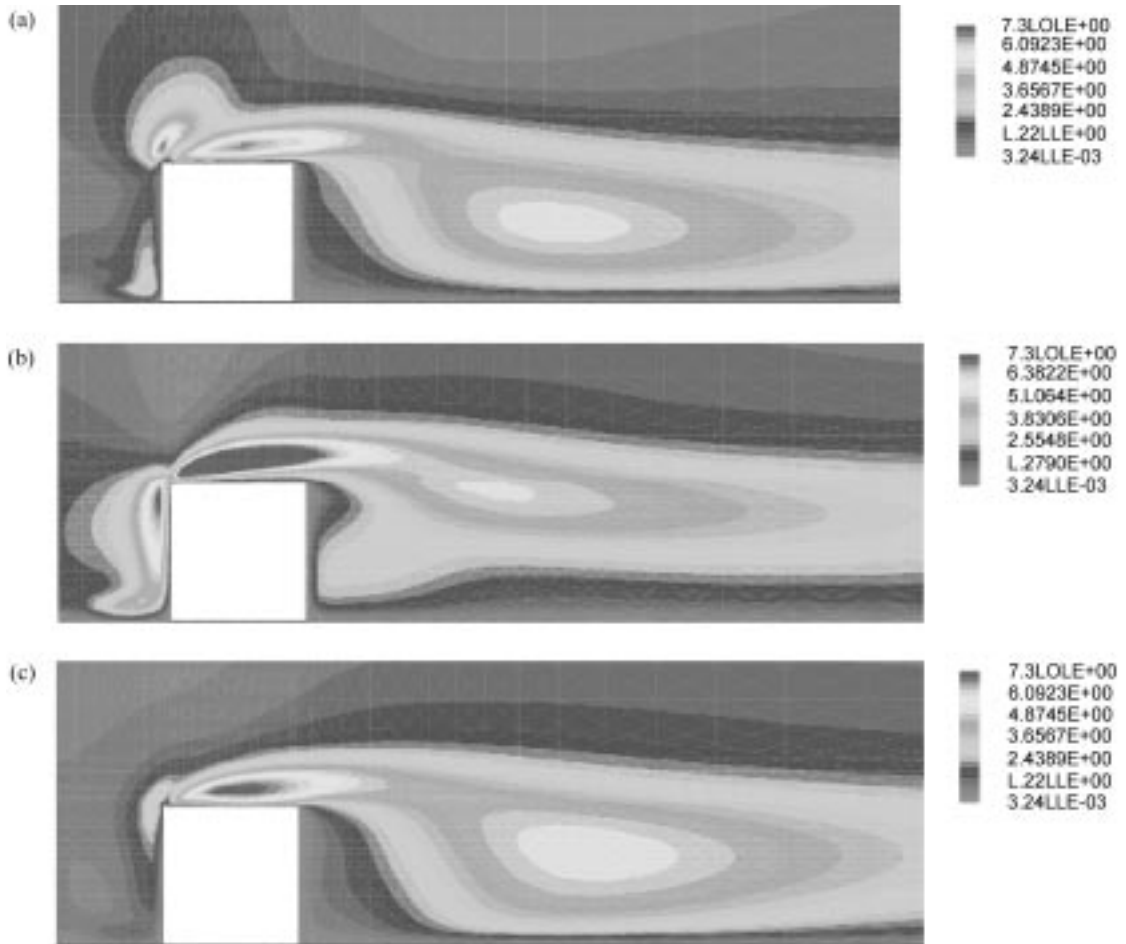


Fig. 15 (a-c) - Reynolds stresses ( $u'u'$ ,  $v'v'$ ,  $w'w'$ ) from the non-linear  $k-\epsilon$  model

of turbulent kinetic energy produced at the front face stagnation point. Consequently it is interesting to see that although the non-linear model predicts a lower level of kinetic energy than the RNG (see Fig. 14) model it still predicts a shorter more accurate roof vortex. This is most likely due to the increased lateral diffusion predicted by the model due to its anisotropic turbulence modelling abilities and the increased levels of shear stress returned as discussed. The same argument also applies to the wake region. Improvements over the standard  $k-\epsilon$  are also apparent for both the velocity and pressure distributions obtained from the skewed cube although it should be noted that no improvement is apparent over the RNG model for this case.

Given that the differential stress model is a fully anisotropic turbulence model it is rather surprising to find that it does not predict a very accurate roof flow field. The reason for the poor roof flow field may be due to the omission of wall reflection terms in the pressure strain model. These are omitted due to the fact that there is no generic way of incorporating these terms for all the different model geometries encountered (further discussion of this is given in Wright and Easom 1999). Another problem in using the DSM is the lack of computational stability of the model in complex flow fields. Nevertheless although the roof recirculation zone is poorly predicted with the

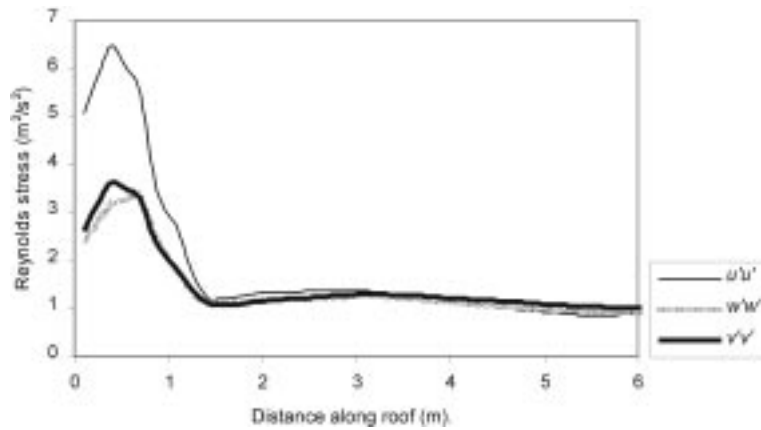


Fig. 16 Normal Reynolds stress distribution for the roof of the 6 m cube calculated using the non-linear  $k-\epsilon$  model

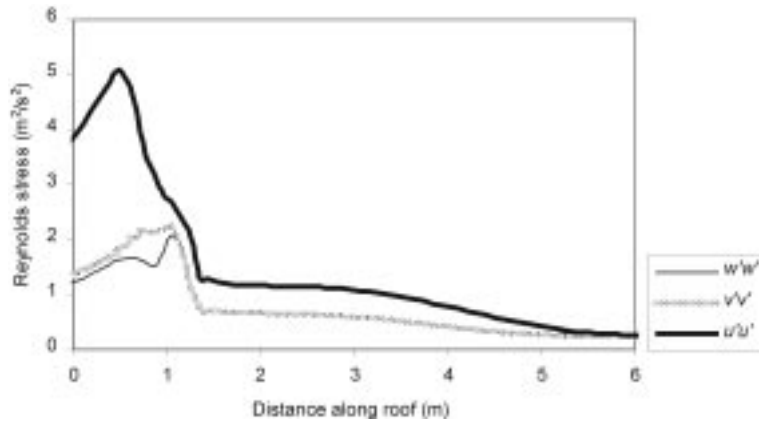


Fig. 17 Normal Reynolds stress distribution for the roof of the 6 m cube calculated using the differential stress model

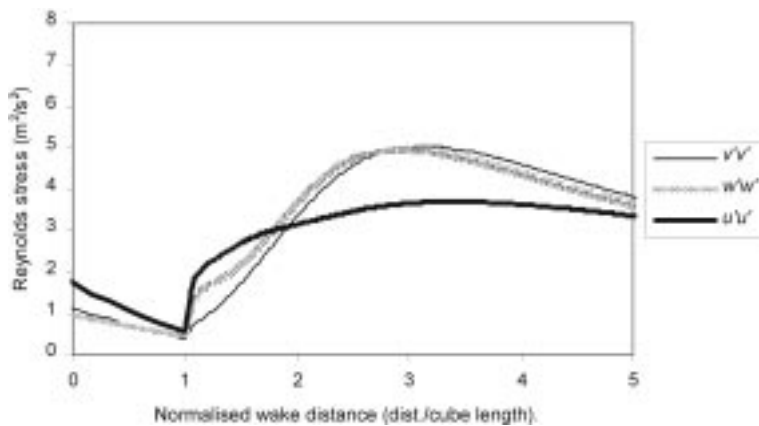


Fig. 18 Normal Reynolds stress distribution for the wake of the 6 m cube calculated using the non-linear  $k-\epsilon$  model

differential stress model the wake recirculation is accurate and the mean pressure coefficients are well predicted. This model also predicted the strongest delta wing vortices. It appears that this model may need some modifications to improve its performance and stability to be fully utilised in wind engineering applications.

## 6. Conclusions

The essential requirements for turbulence modelling in wind engineering flow fields are turbulence anisotropy, computational stability and accuracy.

Isotropic turbulence models such as the standard  $k-\varepsilon$  model have quite rightly come under a lot of criticism due to their flawed assumptions and consequent lack of accuracy when used for bluff body flow fields. Accurate anisotropic models such as the differential stress model and algebraic stress model have rarely been used due to their poor numerical stability and high computational overheads. The results presented here show that the non-linear  $k-\varepsilon$  model that incorporates better anisotropic turbulence modelling and high computational stability and fast solution times takes us one step closer to a usable and accurate turbulence model for wind engineering. This model combines the best features of a number of turbulence models. Furthermore future development work to make higher order non-linear models more stable should ensure even greater accuracy with this type of turbulence model.

Despite the improvements from the non-linear model significant errors were found in the prediction of the pressure distributions. This is likely to be due to the complexity of the flow and the steady state assumption of the CFD. As a consequences the authors have undertaken simulations using large eddy simulation which will be presented elsewhere.

## Acknowledgements

Both authors would like to thank CFX International for allowing the use of the source code for CFX.

Gary Easom would like to thank the Silsoe Research Institute and the University of Nottingham for their financial support during his Ph.D. studies.

## References

- Baetke, F and Werner, H. (1990), "Numerical simulation of turbulent flow over surface mounted obstacles with sharp edges and corners", *J. Wind Eng. Ind. Aerod.*, **35**, 129-147, Elsevier, Amsterdam, Netherlands.
- Basora, B. and Younis, B.A. (1992), "Progress in the prediction of turbulent wind loading on buildings", *J. Wind Eng. Ind. Aerod.*, **41-44**, 2863-2874, Elsevier, Amsterdam, Netherlands.
- Boussinesq, T.V. (1877), *Mem. Pre. Acad. Sci.*, 3rd Edn., Paris XXIII, 46.
- Bradshaw, P. (1973), "Effects of streamline curvature on turbulent flow", AGARDograph no. 169.
- Bradshaw, P. (1992), "Turbulence: the chief outstanding difficulty of our subject", *5th Symp. on Numer. & Phys. Aspects of Aerod. Fl.*, January 1992, California State Univ., USA.
- Craft, T.J. and Launder, B.E. (1972), "New wall reflection model applied to the turbulent impinging jet", *AIAA J.*, **30**, 2970.
- Craft, T.J., Launder, B.E. and Suga, K. (1993), "Development and application of a cubic eddy-viscosity model of turbulence", *Int. J. Heat Fluid Fl.*, **17**: 108-115, 1996, Elsevier Science Inc., New York, USA.
- Easom, G.J. (1997), "Improved computational models for wind engineering", Internal Report No. FR97 016, School of Civil Engineering, The University of Nottingham, UK, (<http://www.nottingham.ac.uk/~evzngw/download.htm>).

- Gaskell, P.H. and Lau, A.K.C. (1988), "Curvature compensated convective transport : SMART, a new boundness preserving transport algorithm", *Int. J. Numer. Meth. Eng.*, **8**, 617-641.
- Hoxey, R., Short, L. and Richards, P. (1999), "Quasi-steady theory developed with experimental verification", *Proc. of the 10<sup>th</sup> ICWE*, Copenhagen 1999, **3**, 1679-1692.
- Kim, J., Kline, S.J. and Johnston, J.P. (1980), "Investigation of a reattaching turbulent flow over a backward facing step", *Transactions of the ASME*, **102**, September 1980.
- Launder, B.E and Spalding, D.B. (1974), "The numerical computation of turbulent flows", *Comput. Methods. Appl. Mech. Eng.*, **3**, 269-289.
- Launder, B.E., Reece, G.J. and Rodi, W. (1975), "Progress in the development of a Reynolds Stress turbulence closure", *J. Fluid Mech.*, **68**, Pt 3, 537-566.
- Leschziner, M.A. (1995), "Modelling turbulence in physically complex flows", Industrial Hydraulics and Multiphase flows - Hydro 2000, Thomas Telford, London, England.
- Lumley, J. (1970), "Towards a turbulent constitutive relation", *J. Fluid Mech.*, **41**, 413.
- Menter, F. and Grotjans, H. (1999), "Application of advanced turbulence models to complex industrial flows", Internal Report, CFX International.
- Murakami, S. (1993), "Comparison of various turbulence models applied to a bluff body", *J. Wind Eng. Ind. Aerod.*, **46 & 47**, 21-36, Elsevier, Amsterdam, Netherlands.
- Murakami, S. (1997), "Overview of turbulence models applied in CWE", Institute of Ind. Science., Univ. Tokyo, Japan.
- Murakami, S., Mochida, A. and Ooka, R. (1993), "Numerical simulation of flow fields over a surface-mounted cube with various second-moment closure models", *Ninth Symp. on Turbulent Shear Flows*, Kyoto, Japan.
- Ng, K.H. (1971), "Predictions of turbulent boundary-layer developments using a two-equation model of turbulence", Ph.D Thesis, University of London, UK.
- Orzag, S.A (1994), Lecture notes of ICASE/LaRC short course on Turbulence Modeling & Prediction, March 1994 in Gatski T.B, Hussaini M.Y & Lumley J.L 1996, "Simulation and Modeling of Turbulent Flows", Oxford University Press, Oxford, England.
- Pope, S.B. (1975), "A more general effective-viscosity hypothesis", *J. Fluid Mech.*, **72**, pt. 2, 331-340.
- Richards, P.J. and Hoxey, R.P. (1993), "Appropriate boundary conditions for computational wind engineering models using the  $k$  -  $\epsilon$  turbulence model", *J. Wind Eng. Ind. Aerod.*, **46-47**, 145-153.
- Rodi, W. (1972), "The prediction of free turbulent boundary layers by use of a two equation model of turbulence", Ph.D. Thesis, University of London, UK.
- Smagorinsky, J.S. (1963), "General circulation experiments with primitive equations, Part 1; basic experiments", *Mon. Weather Rev.*, **91**, 99-164.
- Spalding, D.B. (1972), "A novel finite difference formulation for differential expressions involving both the first and second derivatives", *Int. J. Numer. Meth. Eng.*, **4**, 551.
- Speziale, C.G. (1987), "On non-linear  $k$ - $l$  and  $k$ - $\epsilon$  models of turbulence", *J. Fluid Mech.*, **178**, 459-475.
- Speziale, C.G. and Ngo, T. (1988), "Numerical solution of turbulent flow past a backward facing step using a nonlinear  $k$ - $\epsilon$  model", *Int. J. Eng. Sci.*, **26**(10), 1099-1112.
- Suga, K. (1996), "Development and application of a non-linear eddy viscosity model sensitized to stress and strain invariants", Ph.D. Thesis, Department of Mechanical Engineering, UMIST TDF/95/11.
- Tsuchiya, M., Murakami, S., Mochida, A., Kondo, K. and Ishida, Y. (1996), "Development of a New  $k$ - $\epsilon$  Model for flow & pressure fields around a bluff body", CWE96, *Second Int. Symp. on CWE*, Colorado State University, USA.
- Wilcox, D.C. (1994), "Turbulence modeling for CFD", DCW Industries Inc., Canada.
- Wright, N.G. and Easom, G.J. (1999), "Comparison of several computational turbulence models with full-scale measurements of flow around a building", *Wind and Structures, An Int. J.* **2**(4).
- Yakhot, V., Orsag, S.A.,Thamgam, S., Gatski, T.B. and Speziale, C.G. (1992), "Development of turbulence models for shear flows by a double expansion technique", *Phys. Fluids A*, **4**, 1510-1520.

## Notation

$U_i$	: $i$ th component of velocity
$U_{ref}$	: reference velocity, taken here at a height of 6 m
$k$	: turbulent kinetic energy, $k = 1/2(\overline{u'_i u'_i})$
$\varepsilon$	: dissipation rate of $k$
$P$	: pressure
$\rho$	: fluid density
$\tau_{ij}$	: Reynolds stress tensor
$\sigma_k, \sigma_\varepsilon$	: turbulent Prandtl number for $k$ and $\varepsilon$ for the $k$ - $\varepsilon$ turbulence model
$\mu_t$	: dynamic eddy viscosity
$\nu_t$	: kinematic eddy viscosity
$S_{ij}$	: strain rate tensor
$\delta_{ij}$	: Kronecker delta
$\overline{u'_i u'_j}$	: Reynolds stresses
$P_k$	: production of $k$
$C_{\varepsilon 1}, C_{\varepsilon 2}, C_{1RNG}, C_\mu$	: constants in the turbulence transport equations
$\Omega$	: vorticity
$S$	: shear
$C_{ij}$	: convection term of $\overline{u'_i u'_j}$
$D_{ij}$	: diffusion term of $\overline{u'_i u'_j}$
$F_{ij}$	: stress production of $\overline{u'_i u'_j}$ by action of rotational or body forces
$\phi_{ij}$	: pressure-strain correlation term
$\varepsilon_{ij}$	: dissipation term of $\overline{u'_i u'_j}$

GS